NORWEGIAN JOURNAL OF GEOLOGY
https://dx.doi.org/10.1785/njg101-4-2

GEOLOGICAL SOCIETY OF NORWAY

Caprock integrity of the Draupne Formation, Ling Depression, North Sea, Norway

Roy H. Gabrielsen[1], Elin Skurtveit[2] & Jan Inge Faleide[1]

[1]*Department of geoscience, University of Oslo P.O.Box 1047, 0316 Oslo*
[2]*Norwegian Geotechnical Institute, P.O.Box3930, Ullevål Stadion, 0806 Oslo*

E-mail corresponding author (Roy H. Gabrielsen): r.h.gabrielsen@geo.uio.no

Keywords:
- *Northern North Sea*
- *Draupne Formation*
- *Caprock integrity fracture network*
- *Slickenside*
- *Carbon sequestration (CCS)*

Received:
16. March 2020

Accepted:
10. October 2020

Published online:
24. February 2021

The Draupne Formation is the most important source and cap rock for North Sea hydrocarbon plays. It also provides the primary seal for potential CO_2 storage on the Norwegian Continental Shelf, but it has been a concern that in situ fracturing may compromise its sealing capacity on both regional and local scales. To evaluate its integrity, mudrocks of the Draupne Formation were cored for mapping and analysis of fracture systems in well 16/8–3S. This well was drilled in the Ling Depression of the central North Sea. The background permeability of the Draupne Formation ranges between 10^{-6} and 10^{-3} mD, making it a good caprock for carbon sequestration (CCS). In the 16/8–3S well site, the Draupne Formation is affected by four fracture populations. *Fracture population FP1* consists of bedding-parallel fractures reflecting a mechanical strength anisotropy associated with deposition, and probably exaggerated by the effects of diagenetic processes. *Fracture population FP2* consists of high-angle pedogenic fractures likely reflecting deformation associated with deposition and burial. *Fracture population FP3* consists of inclined (35–60^0) fractures decorated by different types of slickenlines, whereas *Fracture population FP4* is regarded as comprising drilling- and core-handling-induced fractures. The bedding-parallel FP1 population is likely to remain closed for fluid conductivity at depth since the stress caused by the overburden likely exceeds the fluid pressure at the top reservoir level. The FP2 is lithostratigraphically restricted and stratabound and therefore cannot contribute significantly to a three-dimensionally connected network. Potential fluid flow is therefore likely to be constrained to the inclined tectonic fracture population (FP3), which is unlikely to connect in three dimensions due to its low fracture frequency unless the FP1 population had become activated by processes such as unloading. Substantial leakage through the Draupne Formation mudstone related to the observed fracture sets is therefore considered unlikely. It is emphasised that injection of CO_2 would require fluid pressure control at the reservoir-caprock interface to avoid opening of existing fracture populations, induce (new) or reactivate old fracture systems and thereby corrupting the integrity of the seal.

Gabrielsen, R.H, Skurtveit, E. & Faleide, J.I. 2020: Caprock integrity of the Draupne Formation, Ling Depression, North Sea, Norway. ***Norwegian Journal of Geology 100,*** 202019. https://dx.doi.org/10.17850/njg100-4-2.

Introduction

The Draupne Formation, which is composed mainly of mudstone, is the most important source and cap rock for North Sea hydrocarbon systems, and accordingly is of great relevance for the assessment of structures for potential storage of CO_2 in Triassic–Jurassic sandstone reservoirs in this area (Halland et al., 2011; Skurtveit et al., 2015a). Consolidated mudstone and shale have very low hydraulic conductivity and are vulnerable to compaction (Bjørlykke, 1998; Mondol et al., 2007; Avseth et al., 2010 and references therein). It encompasses two principal types of seals: *Membrane seals* fail where net buoyancy pressure exceeds the capillary pressure, and are independent of caprock thickness. In contrast, *hydraulic seals* fail by fracturing before the maximum buoyancy pressure is obtained, and are dependent on caprock thickness (Watts, 1987; Caillet, 1993). Dilational fracture systems can, however, significantly enhance fluid flow capacity in hydraulic seals (e.g., Sibson, 1990 Dehandschutter et al., 2005; Gale et al., 2014; Rutter et al., 2017; Yarushina, 2018), and the mapping of fracture systems is therefore crucial in the evaluation of caprock integrity (e.g., Horsrud et al., 1998; Nelson, 2001; Ross & Boustin, 2008; Loucks et al., 2009; Skurveit et al., 2012; Gale et al., 2014; Ougier-Simonin et al., 2016). It has gained some attention in connection with carbon sequestration (Carbon capture and storage; CCS) (Makurat et al., 1992; Luo & Vasseur, 1997; Camac et al., 2009; Halland et al., 2011; Skurtveit et al., 2012, 2015b; Yarushima, 2018), in connection with the production of shale gas (e.g., Hill & Nelson, 2000; Curtis 2002; Ladéveze et al., 2018), and in the containment of radioactive waste (Green, 1988; Harrington et al. ,2017).

Considering their critical influence on seal integrity in geological reservoirs, fractures in mudstone and shale have gained little attention. This may be related to the diverse nature of fracture systems and the variability of mechanical properties in such lithology, which makes the system difficult to assess (Aplin & Larter, 2005; Hermanrud et al., 2005; see also summaries in Boult & Kaldi, 2005; Wood, 2010a,b; Warren et al., 2010; Rutter & Mecklenburgh 2017; Gale et al. 2014; Ougier-Simonin et al., 2016). The very fine grain-size and variable ductile properties of clays also makes structural studies challenging (Means, 1987; van den Berg, 1987; Power & Tullis, 1989; Will & Wilson, 1989; Wilson & Will, 1990; Gale et al., 2014). These knowledge gaps motivated coring of the Draupne Formation in well 16/8–3S of the Ling Depression at the eastern margin of the Viking Graben of the North Sea (Fig. 1). Well 16/8–3S is an exploration well from 2013 targeting the Permian Rotliegendes sandstones. The well was dry and permanently abandoned. In the present work, the findings from structural investigations of fracture populations and systems on the macro- and micro-scales, and their potential influence on fluid transport are discussed.

The Draupne Formation mudstone

The Draupne Formation of the Viking Group (Vollset & Doré, 1984) in the North Sea is a late Jurassic (Oxfordian–Tithonian; Ryazanian) (Fig. 2), late syn-rift to post-rift low-energy, marine, black, (commonly) fissile mudstone. It is equivalent to the Kimmeridge Clay Formation, which is found in southern and eastern England and in the British sector of the North Sea (e.g., Barnard & Cooper, 1981; Vollset & Doré, 1984; Brown, 1990; Cornford, 2018). The Draupne Formation was deposited in the late syn-rift(?) to early post-rift stage of the development of the Viking Graben system during the Oxfordian–Tithonian (*sensu* IUGS, 2018) and/or Ryazanian (Deegan & Scull, 1977 Whitbread, 1975; Badley et al., 1984; Vollset & Doré, 1984; Gabrielsen et al., 1990, 2001; Nøttvedt et al., 1995; Fraser et al., 2003), and deposited in a low-energy, marine environment (Barnard & Cooper, 1981).

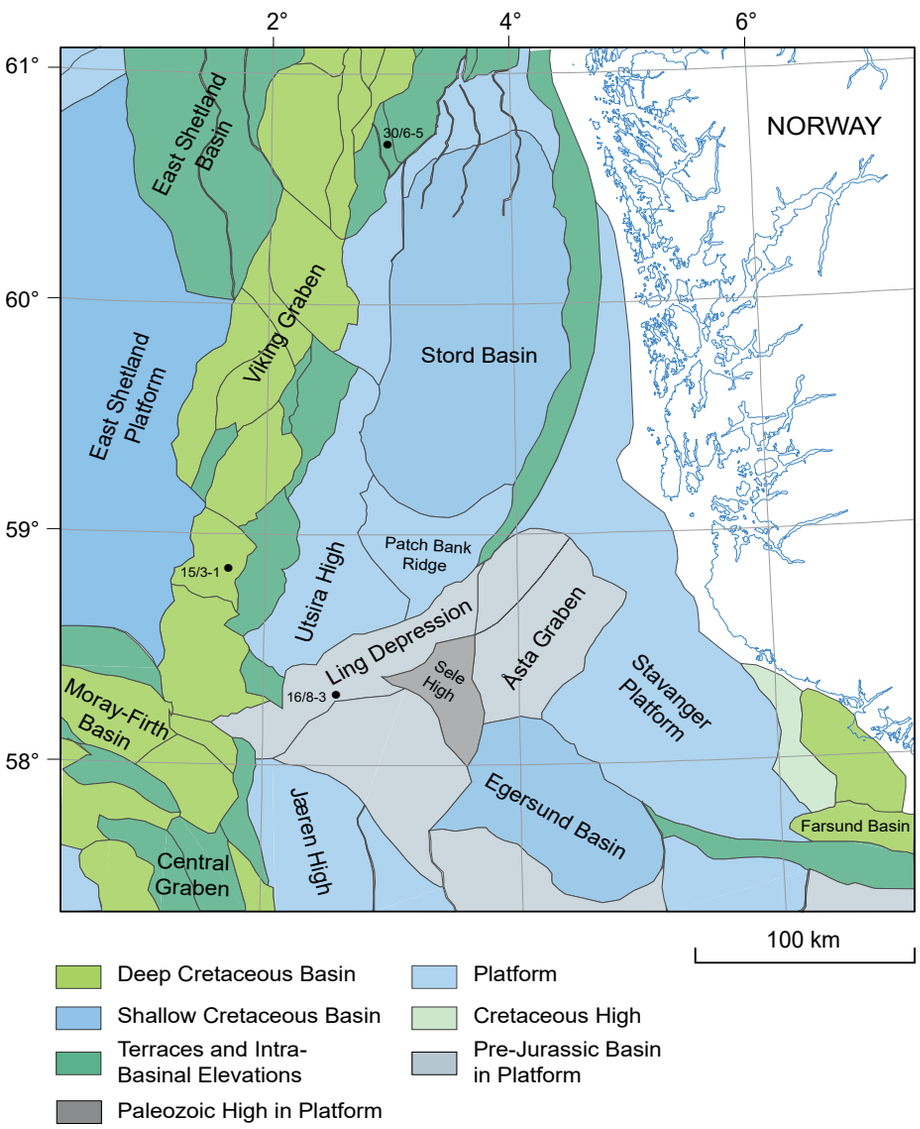

Figure 1. Structural element map of the northern North Sea with locations of wells 30/6–5 (reference wells for Draupne Formation; see text) and wells 15/3–S1 16/8–3S (this study).

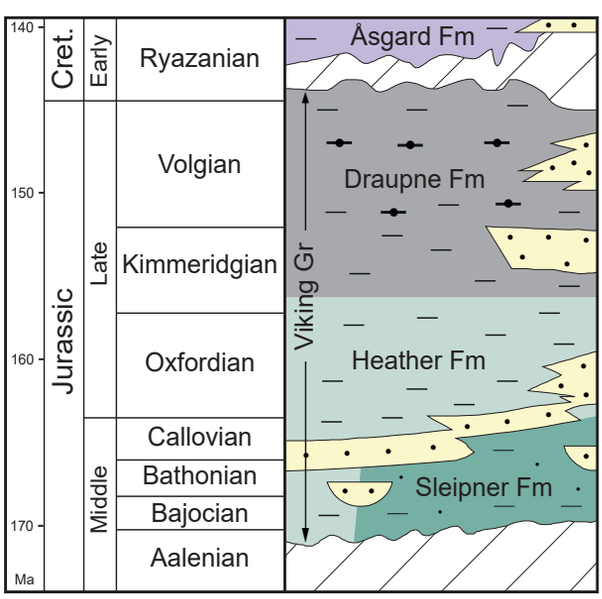

Figure 2. Lithostratigraphic column, Norwegian North Sea. Modified from Norwegian Petroleum Directorate (2014).

The Draupne Formation mudrock is organic rich, radioactive (commonly more than 100 API units; Vollset & Doré. 1984) and is commonly carbonaceous. It locally contains stringers of limestone, siltstone and sandstone of assumed turbiditic origin. It is characterised by anomalously low velocity and high resistivity and is ubiquitous in the northern North Sea, including the East Shetland Basin, the Viking Graben proper and the Horda Platform. It is, however, thinned or absent in some high-standing platforms and at the crests of some rotated/uplifted fault blocks (Gabrielsen et al., 2001; Kyrkjebø et al., 2004). The Draupne Formation mudrock is 163 m thick in the type well (30/6–5) in the Oseberg area, increasing to a maximum of 867 m in well 15/3–S1 of the Gudrun Field on a downthrown subplatform at the eastern flank of the Viking Graben.

A three-fold subdivision of the Draupne Formation, based on contrasts in gamma-ray response, is possible in some places, and particularly so along the basin margins (Vollset & Doré, 1984). Due to the widespread distribution of the formation and the fact that it straddles the syn-rift/post-rift transition of the Viking Graben, the Draupne Formation has a diachronous stratigraphical basal contact (Vollset & Doré, 1984; Gabrielsen et al., 2001, Kyrkjebø et al., 2004). Conceptual and experimental investigations of hydrocarbon leakage, CO_2 breakthrough and flow mechanism were performed by Skurtveit et al., (2012). They estimated a CO_2 breakthrough pressure of 3.5–4.3 MPa and identified micro-fractures as a potential flow path in the rock. Flow mechanism and permeabilities in the Draupne mudstone have not been widely reported in the literature. However, experimental studies of Draupne Formation mudstone from the Troll area found an effective CO_2 permeability in the order of 10^{-6} mD (Skurtveit et al., 2012) which is of the same order of magnitude as the brine permeability in the study area, whereas for core samples from Ling Depression the permeability is reported in the order of 10^{-7} mD (10^{-22} m^2) (Skurtveit et al. 2015b). Nordgård Bolås et al. (2005) reported typical properties of sealing rock units between 10^{-6} and 10^{-3} mD. In particular it is noted that the background permeability of the Draupne Formation mudrocks in the Ling Depression is lower in the Troll area, likely related to deeper burial and compaction.

Core handling and sample selection

One core (Fig. 3) was recovered from the mudstone of the upper Draupne Formation following procedures recommended by Gabrielsen (1997) and Hettama et al. (2002). The coring and sampling process was closely monitored at all stages to ensure an opening process that prevented damage to the core material, Prior to opening, the core was surveyed using a CT-scan, which revealed a generally homogeneous texture with some fractures and restricted rubble zones. This part of the investigation was supported by use of the gamma-ray log. Thus, the sealed core was opened under controlled laboratory conditions and logged at the Norwegian Geotechnical Institute in Oslo. The core naturally separated along bedding-parallel fractures into 10–40 cm-long segments. In order to preserve mechanical properties and to avoid mineralogical reaction with the air, the cores were placed in tight, oil-filled containers and sealed for future study.

Core inspection from the CT-scan and the gamma log provided the basis for selection of the first four core segments to be opened. Following the CT-scanning, four parts of the 16/8–3S core were considered for detailed structural/geomechanical analysis. These were Core segment No. 1 (2574.50–2575.50 m core depth), Core segment No. 2 (2576.50–2577.50 m core depth), Core segment No 8 (2518.50–2582.50 m core depth) and Core segment No. 9 (2582.50–2583.50 m core depth). The uppermost core sections (Core segments No. 1 and 2) were characterised by the lowest gamma-ray log values. These cores displayed fractures of varying geometry and with smooth to heavily decorated surfaces. The two lowermost sections, (Core segments No. 8 and 9), representing the higher gamma-ray log values, showed that Core segments No. 8 and 9 have no structures of tectonic origin beyond a few open, bedding-parallel (FP1)-fractures assumed to be associated with unloading and core opening, and those were accordingly assumed to be tectonically undisturbed. Cores segments No.1 and 2 were therefore selected for fracture studies.

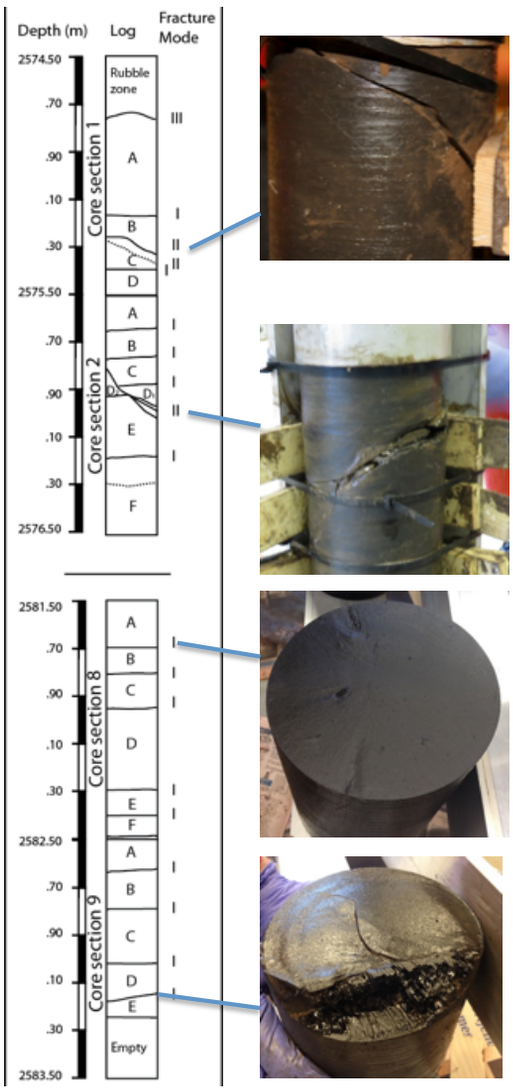

Figure 3. Simplified fracture log and photographs of selected parts of the cored interval from well 16/8–3S.

Mineralogy and geochemistry of the Draupne Formation mudstone

Thirteen samples from the Draupne Formation mudrock in well 16/8–S3 were selected for mineralogical and chemical study including grain-size analysis. Total organic content (TOC) analyses of the samples were performed by Applied Petroleum Technology AS by the application of a Leco SC-632 instrument. Carbonates were removed and carbon dioxide was measured by infrared detection. Mineral composition was analysed by use of x-ray diffraction using a Bruker D8 Advance diffractometer. Physical and direct mineral identification was performed by use of a JEOL JSM-6460 LV scanning electron microscope and samples were inspected under a petrographic microscope coupled with an ultraviolet light source for the detection of the fluorescence of organic matter (Ogebule, 2015).

It is well established that the presence of organic material strongly influences the mechanical properties of mudstone and shale (e.g., Horsrud et al., 1998; Chang et al., 2006), although the relationship between quartz content and TOC remains somewhat obscure (Ougier-Simonin et al., 2016). The TOC of the Draupne Formation generally varies between 100 and well above 350 mg HC/g (Keym et al., 2006).

Optical microscope images taken under ultraviolet light and plane-polarised light (Fig. 4) show variable texture including a dominantly platy to fibrous clay matrix. The mineralogical analysis of the cored interval of well 16/8-3S shows that the mudstone is composed of quartz, albite, microcline, carbonates (calcite, siderite and ankerite), hematite and clay minerals (kaolinite, smectite, illite-smectite, illite and chlorite-smectite). The predominant clay mineral is kaolinite with a maximum of approximately 80% and a minimum of approximately 60% of the total clay content, whereas illite constitutes 8 to 12%, smectite 8 to 23%, mixed layer illite-smectite 7 to 15%, mixed layer chlorite-smectite 8 to 14% and chlorite <2% of the total. The content of albite, hematite, siderite and chlorite-smectite is particularly high in and close to rubble zones in siltstone. Smectite and mixed-layer illite-smectite are concentrated along the slickensides. The clay content increases in the rubble zone, whereas it remains constant or is reduced on fracture surfaces. Intact shale has a TOC content between 6 and 8%.

Well 16/8-3S drilled the Upper Jurassic Draupne Formation within the Ling Graben in the central North Sea (Fig. 1). A core with a diameter of 133 mm was cut at a depth between 2574.5 m and 2583.5 m MD, covering the top of the 86 m-thick Draupne Formation. The main objective was to provide high-quality core for structural and rock mechanical study to assess the seal integrity for potential future CO_2 storage sites in the North Sea.

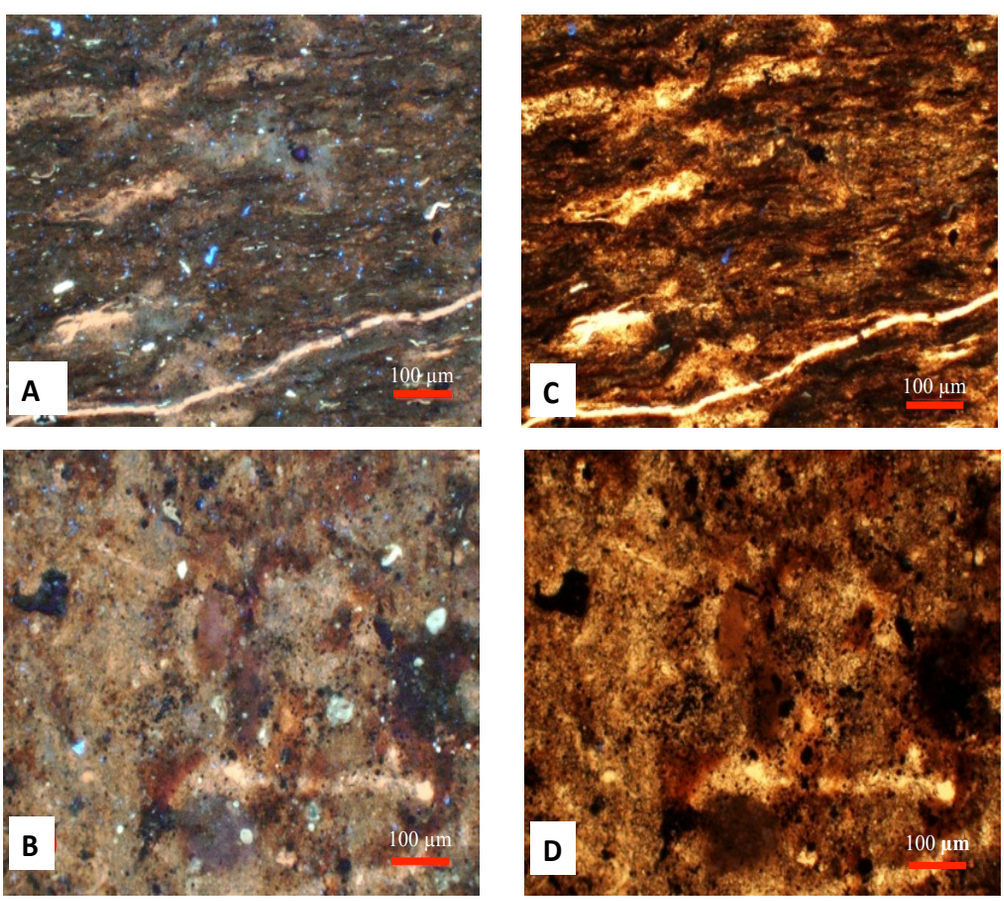

Figure 4. Photomicrographs of the Draupne Formation mudstone in Well 16/8–3S. Sample depth is 2582.50. Sections were cut both perpendicular (A, C) and parallel (B, D) to bedding. The sections are shown in ultraviolet light (A, B) and plane- polarised light (C, D). Pale blue grains represent organic matter. Scale bar = 100 µm.

Fracture description

Fracture frequency, fracture orientation, morphology and decoration of fracture surfaces (strain markers) were applied in the fracture description and classification. Altogether four fracture populations (FP1-FP4) were identified. It is clear that the Draupne Formation core in well 16/8– shows a bulk fracture frequency of 6.5 fractures per cored metre, which is considered moderate, and is affected by fracturing to a very limited degree, but still includes four fracture populations. The bulk fracture frequency is very modest (6.5 fractures per cored metre, including the fracture populations FP1-FP3).

Fracture Population FP1 consists of bedding-parallel fractures, similar to those described in the Draupne Formation mudrocks in the Troll East area of the northern part of the North Sea (Skurtveit et al., 2012). The average fracture frequency (F_f) for the FP1 population is 5.25 fractures/m. FP1 fracture surfaces are generally very smooth, and in places exhibit a bright lustre (Fig. 5A, B). Secondary drying cracks appeared on some FP1 surfaces within minutes after opening of the core in some cases (Fig. 5C). FP1 fractures with flaky surfaces are occasionally seen (Fig. 5D). The flakes are seen at the macro-scale (mm- to cm-scale) as well as on the submicroscopic (200–500 µm) scale. The flakes are generally elliptical to sub-circular in shape and commonly exhibit irregular edges (Fig. 5E, F).

The FP1 fracture population has the characteristics of Mode I-fractures, as they display no indications of bedding-parallel slip. Rock-mechanical experiments (Skurtveit et al., 2015a) confirm that the bedding represents the weakest surfaces in the sediments in that indirect measurements give a tensile strength of 0.1–1.5 MPa for bedding-parallel failure. We suggest that the FP1 fractures reflect primary depositional surfaces that became consolidated during compaction and diagenesis. They become activated by release of the vertical stress during unloading. The mechanical weakness of these planes is also evident from fractures commonly opening during thin-section preparation in this study.

Fracture Population FP2 occurs only in a c. 25 cm-thick siltstone layer at the top of Core segment No.1 This siltstone has previously been considered to belong to the Åsgård Formation situated on top of the

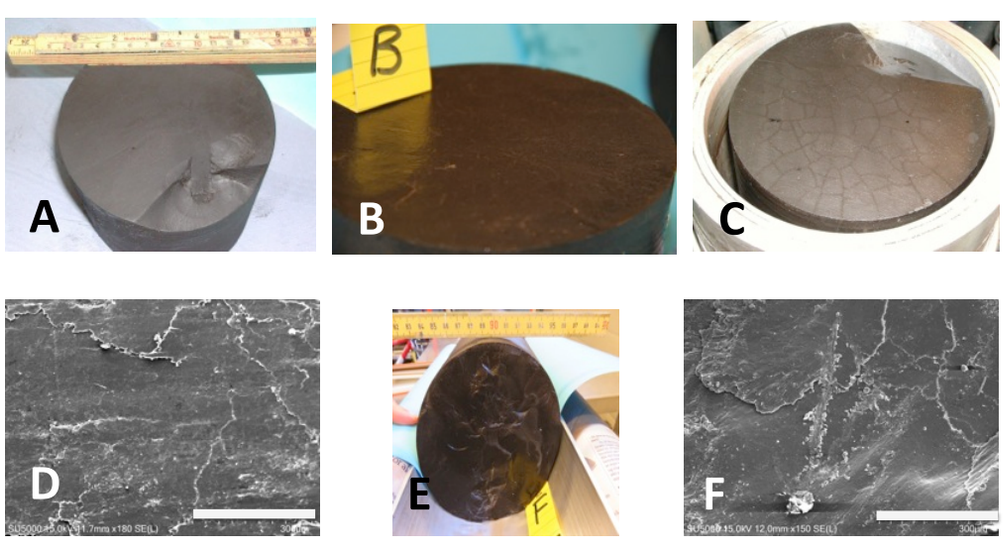

Fracture Popula-on FP1 (S_0)

Figure 5. Examples of fractures belonging to fracture population FP1; Dull (A) and lustrous (B) bedding-parallel fractures, (C) FP1 plane with drying cracks that generated after core opening, (D) SEM image of FP1 plane with a smooth texture, (E, F) Photo and SEM-image of FP1 surface showing a flaky texture. The straight abrasional scar in the central part of figure (F) was probably produced during the core handling. Scale bars (lower right) on SEM-micrographs are 300 µm.

Draupne Formation (Skurtveit et al., 2015a), but more likely represents an intra-Draupne Formation siltstone bed associated with transgression-regression cycles or part of a turbidite sequence (Rawson & Riley, 1982 Vollset & Doré, 1984).

The FP2 fractures are intraformational, i,e., they are exclusively restricted to the siltstone bed and preserved as a rubble zone which forms a collapsed three-dimensional fracture network (Fig. 6A). The fracture population encompasses fractures with planar to irregular geometries. These fractures restrict rock fragments of variable geometry and size (Fig. 6B). The fractures are classified as Mode I-type and are dominantly oriented at a high angle to bedding, although some less steep fractures do occur. The FP2 fractures are likely of pedogenic origin, and were likely influenced by biogenic activity such as burrowing (e.g., Maltman, 1981; Gabrielsen & Aarland, 1990, Gray & Nickelsen, 1989; Gale et al., 2014). The morphology of the fragments, however, is different from lozenge-shaped fragments which are more typical of pedogenic and hydroplastic deformation (Petit, 1987; Gray & Nickelsen, 1989; Gabrielsen & Aarland, 1990; Dehandschutter et al., 2005). Although the majority of the FP2 fractures are now open, the fracture walls reveal that most of them have been filled with carbonate and are surrounded by a dark reddish-brown halo of oxidised country rock (Fig. 6A). This suggests that they were flushed by an oxidising fluid phase (gas or liquid), which has dissolved the carbonate The FP2 fractures were mineralised in situ, possibly in association with compaction and syncompactional water escape.

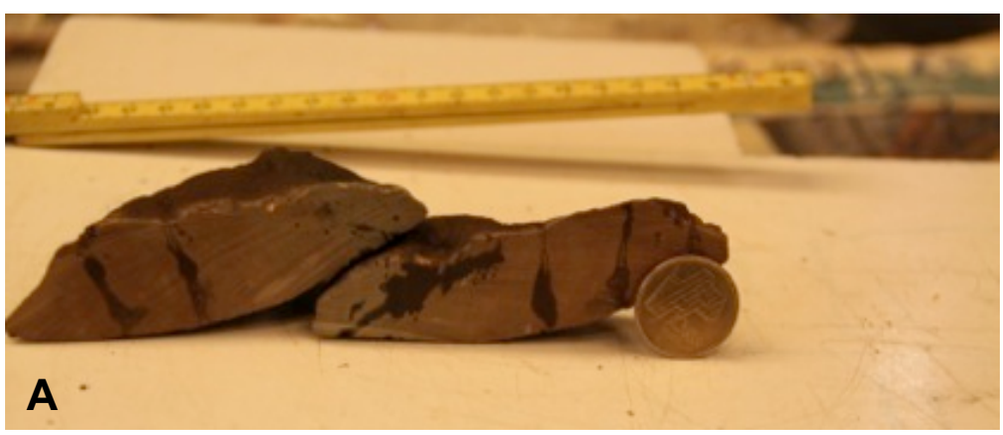

Fracture population FP2

Figure 6. (A) FP2 fractures with carbonate fracture fill. Also note oxidised haloes along fractures. This fracture population is only found intraformationally in siltstone stringers in the upper part of the Draupne Formation. (B) Rubble zone in siltstone layer, which was probably generated by drilling-induced collapse of the FP2 fracture system.

Faint slickenside lineations are found on some siltstone fragments, but these are considered to be drilling-induced. The fracture system was likely opened during drilling and/or core handling. These structures were therefore not given any further attention in this study.

Fracture Population FP3 consists of inclined, planar to sub-planar, slickensided fractures with dip angles between 35° and 60° and with an average F_f of 1.5 fractures/m. The FP3 fractures are characterised by composite planar to slightly undulating surfaces. Some fractures are morphologically composite, including parts of glossy (in places very lustrous) appearance (Fig. 7A–i, B), alternating with segments with a more irregular geometry (Fig. 7A–ii) and hackle marks (e.g., Angelier, 1994 Fig. 7A–iii). They are penetrative on the scale of the core and in places form arrays of (sub)-parallel fractures constituting splays or splay swarms, which define cm-scale lenses, the striated surfaces commonly interfering with more steeply dipping surfaces which show a similar morphological character. These intersections define scoop-shaped surfaces and centimetre-scale lozenge-shaped bodies (Fig. 7A–iv) The scoop-shaped surfaces have a lustrous appearance but may still be covered by very tightly nested slickenlines (Means, 1987; Toy et al., 2017). The largest lens-shaped body displays an a-axis of 6 cm, b-axis of 14 cm and c-axis of 3 cm (for definition of axes in lenses, see Lindanger et al., 2007 Gabrielsen et al., 2017). No correlatable marker beds are affected by the FP3 fractures and therefore it is not possible to determine their offsets.

The FP3 fractures are commonly decorated by a dip-parallel slickenside lineation. Transverse steps and comb marks (Hancock & Barka, 1987) are developed on some, but not all, SP3 surfaces (Fig. 7A–iii, C). Horizontal and oblique lineations also occur but less frequently (Fig. 7C), suggesting a composite development. The slickenside lineations are characteristic of the 'tectonic tool-mark' or abrasional type (e.g., Angelier, 1994 Toy et al., 2017) and occur on the walls of separate mm-thick lamellae likely representing primary local strain features rather than rotational reorientation of one lineation population as described by Twiss et al., (1991).

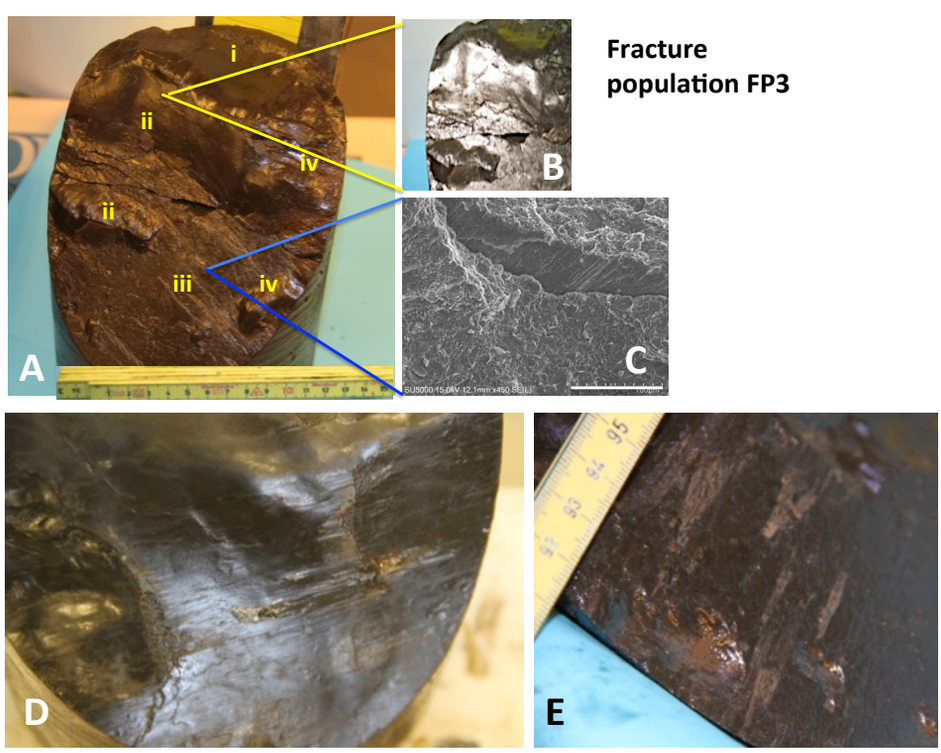

Figure 7. Inclined composite slickenside of fracture population FP3. Note the tendency to form clustered families (arrays) of (sub)-parallel fractures with different morphologies: (A) composite fracture FP3 with areas of contrasting morphology emphasised. (i) smooth mirror area, (ii) irregular mirror area, (iii) abrasion steps and (iv) lens-shaped morphology. (B) Irregular mirror surface seen by oblique illumination emphasising its smooth lustrous property. (C) SEM imagery of abrasion step. Scale bar = 100 µm. (D) Horizontal nested slickenlines on irregular FP3 surface. (E) FP3 surface with spike-shaped calcite slickenfibres.

However, some slickenlines are characterised by a moderate topology and are interpreted to be of the nested type (Means, 1987; Will & Wilson, 1989; Wilson & Wil, 1990; Power & Tullis, 1989). Although these slickenlines can be distinguished on some of the FP3 surfaces, they require the use of a scanning electron microscope (see below).

Finally, some fracture surfaces are decorated by horizontal calcite-slickenfibres (Kirkpatrick & Brodsky, 2014; Toy et al., 2017) (Fig. 7E), which show spike shapes (Will and Wilson, 1989). These can be interpreted as mineral steps related to dip-slip displacement (Angelier, 1994), but their spike shape may rather indicate that localised strike-slip displacement has contributed to this deformation (Will & Wilson, 1989).

The slickenlines on the FP3 fractures can generally be defined visually, but only characterised with confidence using the electron microscope, which can display contrasting morphologies in the presence of striations, slickenlines and slickenfibres (*sensu* Toy et al., 2017; Fig. 7). Images from the electron microscope show that the slickenlines are subdivided into morphological families each including subsets characterised by slightly divergent orientations (deviations of plunge directions by 5° to 15°; Fig. 8A)

The slickenside lineations identified in this study are of the abration type (e.g., Hancock & Barka, 1987; Angelier, 1994 Renard et al., 2012; Toy et al., 2017). Examples where C'-plane truncations and the remnant asperitiy fragments (mainly quartz grains) (Will & Wilson, 1989) are preserved and located at the end points of individual slickenside lineations are common (Fig. 8B). Transverse structures

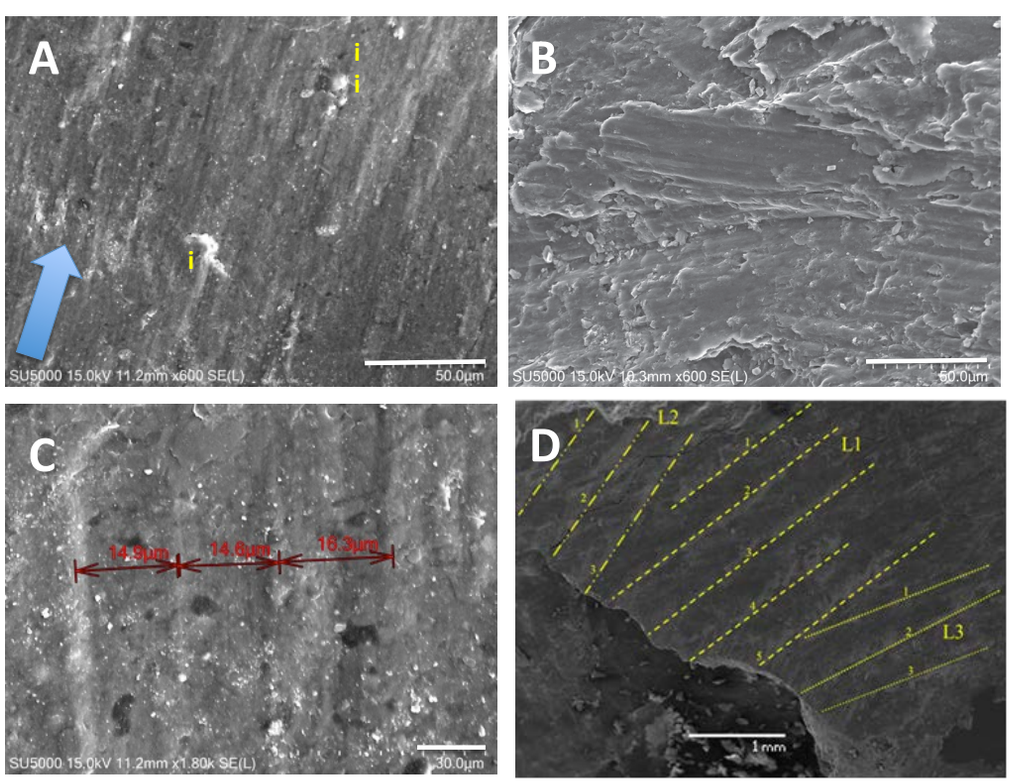

Figure 8. SEM-imagery of slickenside lineations of FP3. (A) Families of nested dip-slip slickenlines on flakes that comprise 'polished' FP3 fractures ('i' in Figure 7). Note divergent slickenline orientation at different flake surfaces. Scale bar is 50 µm. (B) Abrasion slickenside striation remnant with asperity fragments associated with the striae (i: mainly quartz grains) and micro-C'-plane step (ii: white transverse structure). Displacement vector indicated by arrow. Scale bar is 60 µm. (C) Tightly spaced lineations on undulating 'polished' surface (i in Figure 7). The wavelengths of the slickenlines are 15–16 µm. Scale bar in lower right is 30 µm. (D) Sub-families of cross-cutting nested striations on a planar slickenside. Scale bar is 1 mm.

(Hancock & Barka, 1987) also occur in association with these slickenside lineations (Figs. 7B–iv & 8B). These are accordingly of the same type as described from the mudrocks of the Fuglen and Hekkingen formations of the Barents Sea (Gabrielsen & Kløvjan, 1997).

Other slickenside lineations display contrasting mineralogical compositions between ridges (calcite-dominated; Fig. 7E) and depressions (illite-smectite-dominated), alignment of clay particles, more rounded ridges and smaller dimensions (wavelengths of c. 14 μm; Fig. 8C), perhaps generated by expansion and contraction (Gray & Nickelsen, 1989), plastic yielding and strain alignment (Means, 1987; Will & Wilson, 1989; Wilson & Will, 1990; Power & Tullis, 1989). Such processes can produce slickenside lineations of the 'ridge-in-groove' type (Means, 1987) that exceed the amount of fault displacement (Will & Nelson, 1989). They are usually affiliated with thin shaly flakes and in places display subfamilies with divergent orientations (Fig. 8D). No transport direction can be determined for these structures, and it is questionable whether they are associated with shear at all (see Díscussion below).

Fracture Population FP4. Sets of fractures with contrasting attitude that are interpreted as the consequence of drilling and core handling were identified, using the criteria of Arthur et al., 1980; Casey Moore et al., 1986; Brudy & Zoback, 1999 and Tingay et al., 2008). These are here grouped under fracture population FP4. Fracture Population FP4 typically exhibits a conical geometry with the centre of rotation situated in the middle of the core. The FP4 fractures are Mode III structures and are characterised by a concentric pattern of lineations, which suggests a syn-drilling, torsional origin for these structures (e.g., Carson et al., 1982). Given this interpretation, this fracture population is irrelevant for caprock leakage and is given no further attention in this study.

Discussion: The sealing capacity of the Draupne Formation mudrock

The Draupne Formation is the principal source rock and stratigraphic seal for hydrocarbon traps in the North Sea (e.g., Glennie, 1984; Brekke et al., 2001; Kubala et al., 2003; Keym et al., 2006; Cornford, 2018) and thereby also a potential seal for future CO_2 storage (Halland et al., 2011). The Draupne Formation mudrocks are of good caprock quality with matrix permeabilities between 10^{-6} and 10^{-3} mD. The natural fracture (in situ) frequency is low to moderate with a bulk F_f of approximately 6.5 (fractures per metre), of which the bedding-parallel fracture population FP1 is the dominant element with a F_f-value of 5.25. To the extent that the deformation in Well 16/8–3S is representative for the lithological succession, the Draupne Formation mudrocks can therefore be regarded as an excellent caprock for CSS purposes.

The Ling Depression (Brekke et al., 2001; Heeremans & Faleide, 2004) is a part of the North Sea basin system, but defines a less common structural trend of this system in that its basin axis strikes NE–SW. It is flanked by the Utsira and Sele highs to the northwest and southeast, respectively, and is dominated by NE–SW-striking internal and marginal normal faults. The depression is possibly associated with reactivation of the Hardangerfjord shear zone – Midland Valley system and coincides with the northern limit of the Upper Permian salt basins in the area. It is intersected by N–S-striking Mesozoic faults. Although the interior Ling Depression is affected by a number of rotated fault blocks (Heeremans & Faleide, 2004; Khan, 2013), the Jurassic–Cretaceous sequence in the Well 16/8–3S area is not affected by faults that are detectable on the scale of resolution of available reflection seismic data. The fractures observed in the Draupne Formation in the 16/8–3S core are therefore not likely associated with any particular macro-scale fault.

The development of the fracture systems in Well 16/8–3S can also provide information on the burial/uplift history in this part of the Ling Depression. The development of the FP1-fractures was influenced by the primary mineral composition and texture (preferred orientation of platy minerals), which introduced a mechanically defined bedding-parallel inhomogeneity. This mechanical inhomogeneity became exaggerated during diagenesis and generated the mechanically weakest parts of the mudstone. It is therefore concluded that the FP1 population represents a combined primary (sedimentary) and secondary (diagenetic) property of the Draupne Formation. Neither the FP1 nor the FP2 fracture populations are associated with enhanced permeability at the present lithostatic pressure and therefore do not contribute significantly to the in situ permeability. The morphological variability ofthe FP1 population fractures probably reflect subtle contrasts in primary characteristics such as depositional processes, mineral composition and diagenesis (Maltman, 1981; Kisch 1991; Thyberg et al., 2009; Thyberg & Jahren, 2011). These primary characteristics may influence the distribution of larger mineral grains (quartz) and microfractures that generate stress concentrations on the micro-scale (Gale et al., 2014; Ogier-Simonin et al., 2016; Rutter & Meckelburgh, 2017). This is likely to stimulate fracture initiation during the unloading of the core. The measured tensile strength is low (Skurtveit et al., 2015a) and indicates that the vertical load on the FP1 fractures (σv) controls the fracture formation. At the core depth of 2500 m, the least principal stress will be horizontal. There are, however, no indications that the FP1 fractures are open in situ. It is therefore concluded that the FP1 fractures represent dormant structural features associated with burial, uplift and diagenesis, and that the fractures were activated or reactivated during drilling, unloading and core handling.

The FP1 fracture population can only support horizontal CO_2-flow and would only generate efficient leakage of CO_2 in cases where it interferes with fractures of the FP3 population (Fig. 9).

Siltstone stringers are common in the Draupne Formation (e.g., Brown, 1990; Cornford, 2018) and such strata are found at the top of core segment 1 in well 16/8–3S and are the coarsest and most brittle units in the cored sequence. The siltstone hosts the FP2 fracture population that likely represents synsedimentary and compactional deformation. The FP2 fractures were flushed by an active agent that oxidised the fracture walls in an early diagenetic stage, possibly in connection with water-escape. This fracture population, which is exclusive to the siltstone stringers, remained intraformational, and did not affect the mudstone sequence above or below the siltstone (Fig. 9). The influence of the FP2 population on fluid communication is therefore negligible, but its influence may be greater in the more silty parts of the Draupne Formation.

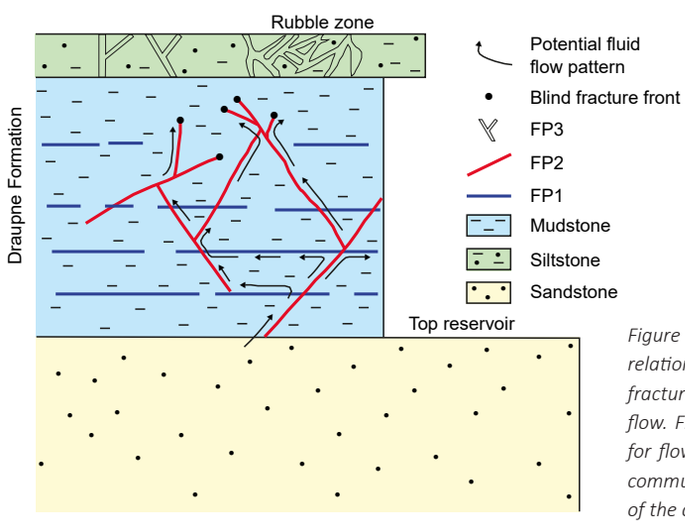

Figure 9. Schematic diagram showing relationship between lithostratigraphy, fracture populations and potential fluid flow. Filled black circles indicate dead ends for flow of CO_2. Note that there is no fluid communication route beyond the lower part of the cap rock.

Though not dateable, it is reasonable to assume that the inclined *FP3 fracture population*, polished or slickenside lineation-decorated, fracture surfaces was initiated during burial and maximum(?) loading of the Draupne Formation during compaction. The fracturing was accompanied by moderate shearing and the development of conjugate fracture sets with incipient nested (ridge-and-groove) slickenlines (Means, 1987; Will & Wilson, 1989; Wilson & Will, 1990; Toy et al., 2017). The core studied herein was taken from a depth of 2574.5–2583.5 m. The maximum burial depth of this core was <3000 m, which was followed by modest uplift (<100 m; Baig et al., 2019). Extrapolating geothermal gradients from Block 17 (Kalani et al., 2015) and ongoing regional studies (Baig et al., 2019) suggest a thermal gradient of 30–35°C/km for the study area. This in turn suggests a temperature at maximal burial of approximately 100°C, which indicates the occurrence of chemical compaction which normally occurs at temperatures >70–80°C (Bjørlykke & Høeg, 1997; Bjørlykke, 1999). It is therefore assumed that slickensides were generated by shear at maximum burial by a stress of approximately 70 MPa ($\sigma v_{max} = \rho g h_{max} = 2.40\ kg/m^3 * 9.81\ km/s^2 * 3 * 10^3\ m$) and temperatures of c. 100°C. By continued moderate shear along the fractures, scoop-shaped structures and lenses were generated and followed by the development of transport-parallel (abrational) striations (*sensu* Toy et al., 2017). The structures converged towards smooth fracture planes ('mirror planes'; Petit, 1987; Power & Tullis, 1989 and Kirkpatrick & Brodsky, 2014), on segments of which different types of slickenside lineations were preserved. *The FP4 fracture population* developed from the effect of drilling and core handling and has accordingly no effect on fluid communication in the Draupne Formation (in situ) caprock.

The structural history of the Draupne Formation, as demonstrated by our analyses of the 16/8–3S core, can therefore be summarised as follows (Fig. 10):

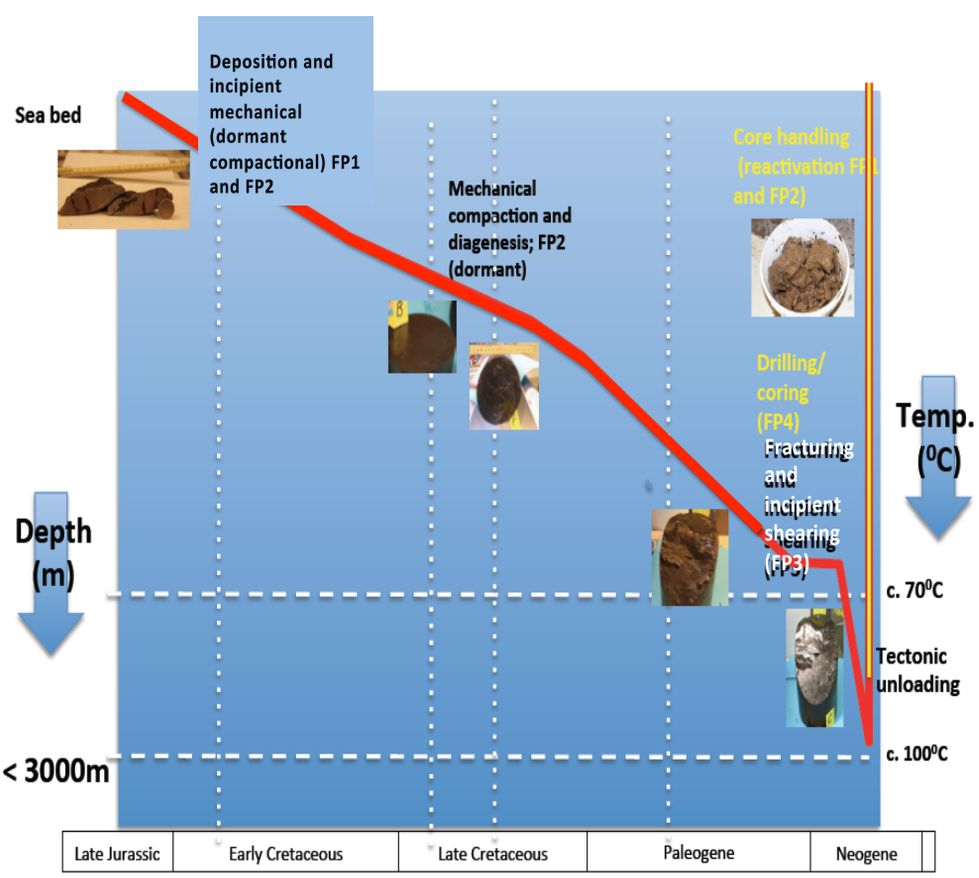

Figure 10. Schematical burial-uplift curve for the Draupne Formation in well 16/8–3S and estimated initiation of fracture populations in the depth/temperature-time space. Red part of the curve illustrates geological burial-uplift, yellow part of the curve indicates 'artificial' uplift of core following drilling. The diagram is not to scale.

1) The deposition of the mud-dominated Draupne Formation and its immediate burial and loading were associated with the development of bedding-parallel fractures due to depositional processes, compaction and rotation of platy minerals into parallelism with bedding. These surfaces served as (cohesive) planes of weakness (FP1) during further burial and unloading

2) Burial and compaction and associated water-escape structures and diagenesis led to incipient fracturing (FP2) and fluid-assisted oxidation of brittle sediments (siltstone).

3) Continued burial was associated with the development of inclined fractures (FP3) in the mudstone, providing a background fracture system, which developed mirror planes and/or slickenside lineations. FP3 fractures may be contemporaneous with post-rift extension-related subsidence of the Viking Graben.

4) Stress release took place during regional uplift.

5) FP4-fracturing occurred during drilling and core handling.

Conclusions

The 16/8–3S core was acquired specifically for the assessment of the caprock integrity of the Draupne Formation. Mudrocks have generally poor primary diffusion properties and the Draupne Formation mudrock falls well inside the typical permeability interval for mudrocks of 10^{-6} to 10^{-3} mD (10^{-21} to 10^{-18} m^2). Even so, petroleum commonly migrates vertically through large thicknesses of fine-grained sediments by diffusion, commonly supported by 3D-interconnected fracture systems (e.g., Aplin & Larter, 2005) and micro-fractures. Previous experiments suggest that both micro-fractures and capillary effects contribute to the build-up of critical pressure for seal integrity, resulting in the formation of channels of enhanced fluid communication, perhaps during formation of micro-cracks (Skurtveit et al., 2012; Harrington et al., 2017). Thre are no indications, however, in the study area that suggest linkage between the observed fracture system and the damage zone of a macroscopic fault. The observed fractures are therefore parts of a background fracture network (Odling et al., 1999; Schueller et al., 2012; Gabrielsen & Braathen, 2014), in which burial and uplift have been the driving mechanisms. The bulk fracture frequency is very modest and not sufficient to generate a connected 3D network that could efficiently support any fluid transport.

This study has shown that the mudstones of the Draupne Formation have suffered a very limited deformation, so that bedding-parallel fractures (FP1 population) are the most common fractures in the investigated cores ($F_f \approx 5.25$). The FP1 fractures have resulted from small compositional/mineralogical contrasts, accumulation of flaky minerals and diagenesis. Also, the incipient flaky quartz fabric was likely formed during early diagenesis (Maltman, 1981; Kisch, 1991; Thyberg & Jahren, 2011). These processes create mechanically weak surfaces along the bedding planes, that are vulnerable to opening by Mode I fracturing when subjected to moderate horizontal (compressional) stress or unloading. They are thereby likely sites for the accumulation of micro-fractures (Power & Tullis, 1989; Will & Wilson, 1989, Wilson & Will, 1990; Kalani et al., 2015; Rutter & Mecklenburgh, 2017) that can potentially enhance horizontal fluid communication.

In conclusion, we have shown that the Draupne Formation mudrock provides an excellent seal for CO_2-storage in areas where its thickness exceeds the critical thickness (Halland et al., 2011). Fracture analysis in the Ling Depression demonstrated that the Draupne Formation has been subjected to only moderate brittle deformation and that its sealing capacity is not compromised by fracturing. Fracturing may, however, be more critical in areas with a varying burial/uplift histories and in the vicinity of major faults.

Acknowledgements. This study is part of the CO2Seal project (Evaluation of the long-term sealing capabilities in the southern Norwegian sector of the North Sea for CO_2 storage purposes) and the JAPSS sub-project (Joint acquisition project for seal samples)—both funded by the CLIMIT programme (Research Council of Norway/Gassnova) and Statoil (now Equinor). We also thank the licence partners Statoil, Dong, Noreco and Wintershall for allowing to use well 16/8–3S for coring the Draupne shale.

The responsibility for conclusions expressed in this paper rest on the authors alone and does not necessarily reflect that of either the CO2Seal-project or the project owners. The paper benefited much from scientific and linguistic comments and advice by an anonymous referee.

References

Angelier, J. 1994: Fault slip analysis and palaeostress reconstruction. *In* Hancock P.L. (ed.): *Continental Deformation,* Pergamon Press, pp. 53–100.

Aplin, A.C. & Larter, S.R. 2005: Fluid flow, pore pressure, wettability, and leakage in mudstone caprocks. *In* Boult, P. & Kaldi, J. (eds.): *Evaluating Fault and Cap Rock Seals,* American Association of Petroleum Geologists, Hedberg Series 2, pp. 1–12.

Arthur, E., Carson, B. & von Huene, R. 1980: *Initial tectonic deformation of hemipelagic sediment at the leading edge of the Japan convergent margin.* Initial Report Deep Sea Drilling Project, Washington D.C., U.S. Government Printing Office 56, 5, part 1, 569–613. https://doi.org/10.2973/dsdp.proc.5657.115.1980.

Avseth, P., Mukerij, T., Mavko, G. & Dvorkin, J., 2010: Rock-physics diagnostics of depositional texture, diagenetic alterations, and reservoir heterogeneity in high-porosity siliclastic sediments and rocks – a review of selected models and suggested work flows. *Geophysics 75,* 75A31–75A47. https://doi.org/10.1190/1.3483770.

Badley, M.E., Egeberg, T. & Nipen, O. 1984: Development of rift basins illustrated by the structural evolution of the Oseberg structure, Block 30/6, offshore Norway. *Journal of the Geological Society of London 141,* 639–649. https://doi.org/10.1144/gsjgs.141.4.0639.

Baig, I., Faleide, J.I., Mondol, N.H. & Jahren, J. 2019: Burial and exhumation history controls on shale compaction and thermal maturity along the Norwegian North Sea basin margin areas. *Marine and Petroleum Geology 104*, 61–85. https://doi.org/10.1016/j.marpetgeo.2019.03.010.

Barnard, P.C, & Cooper, B.S. 1981: Oils and source rocks of the North Sea area, *In* Illing, L.V. & Hobson, G.D (eds.): *Petroleum Geology of the Continental Shelf of NW Europe,* (Institute of Petroleum, London), pp. 169–175.

Bjørlykke, K. 1998: Clay mineral diagenesis in sedimentary basins – a key to the prediction of rock properties. Examples from the North Sea Basin. *Clay Mineralogy 33,* 14–34. https://doi.org/10.1180/claymin.1998.033.1.03.

Bjørlykke, K. 1999: Principal aspects of compaction and fluid flow in mudstones. *Geological Society of London Special Publication 158,* 73–78. https://doi.org/10.1144/GSL.SP.1999.158.01.06.

Bjørlykke, K. & Høeg, K. 1997: Effects of burial diagenesis on stresses: compaction and fluid flow in sedimentary basins. *Marine and Petroleum Geology 41,* 267–276. https://doi.org/10.1016/S0264-8172(96)00051-7.

Boult, P. & Kaldi, J. 2005: *Evaluating Fault and Cap Rock Seals.* American Association of Petroleum Geologists, Hedberg Series 2, 268 pp.

Brekke, H., Sjulstad, H.I., Grogan, P., Magnus, C., Riis, F. & Williams, R. 2001: Sedimentary environments offshore Norway – an overview. *In* Martinsen, I.J. & Dreyer, T. (eds): *Sedimentary Environments offshore Norway; Palaeozoic to Recent.* Norwegian Petroleum Society Special Publication 10, pp. 7–37. https://doi.org/10.1016/S0928-8937(01)80006-0.

Brown, S., 1990: Jurassic. *In* Glennie, K.W. (ed.): *Introduction to the Petroleum Geology of the North Sea,* Third edition, Blackwell Science, pp. 219–254.

Brudy, M. & Zoback, M.D. 1999: Drilling-induced tensile wall-fractures: implications for determination of in-situ stress orientation and magnitude. *International Journal of Rock Mechanics and Mining Sciences 36,* 191–215. https://doi.org/10.1016/S0148-9062(98)00182-X.

Caillet, G. 1993: The caprock of the Snorre Field, Norway: a possible leakage by hydraulic fracturing. *Marine and Petroleum Geology 10*, 42–50. https://doi.org/10.1016/0264-8172(93)90098-D.

Camac, B.A., Hunt, S. & Boult, P.J. 2009: Predicting brittle cap-rock failure of petroleum traps: an application of 2D and 3D distinct element method. *Petroleum Geoscience 15,* 79–89. https://doi.org/10.1144/1354-079309-796.

Carson, B., von Huene, R. & Arthur, M. 1982: Small–scale deformation structures and physical properties related to convergence in Japan Trench slope sediments. *Tectonics 1,* 277–302. https://doi.org/10.1029/TC001i003p00277.

Casey Moore, J., Roeske, S., Lundberg, N., Shoonmaker, J., Cowan, D.S., Gonzales, E. & Lucas, S.E. 1986: Scaly fabrics from Deep Sea Drilling Project cores from forearcs. *Geological Society of America Memoir 166,* 55–73. https://doi.org/10.1130/MEM166-p55.

Chang, C., Zoback, M.D. & Khaksar, A. 2006: Empirical relations between rock strength and physical properties in sedimentary rocks. *Journal of Petroleum Science and Engineering 51,* 223–237. https://doi.org/10.1016/j.petrol.2006.01.003.

Cornford, C. 2018: Petroleum systems of the South Viking Graben. *In* Turner, C.C.& Cronin, B.T. (eds.): *Rift-related coarse-grained submarine fan reservoirs; the Brae Play, South Viking Graben.* American Association of Petroleum Geologists Memoir 115, pp. 453–542. https://doi.org/10.1306/1365219M1153816.

Curtis, J.B. 2002: Fractured shale-gas systems. *American Association of Petroleum Geologists Bulletin 86,* 1921–1938. https://doi.org/10.1306/61EEDDBE-173E-11D7-8645000102C1865D.

Deegan, C.E. & Scull, B.J. 1977: A standard lithostratigraphic nomenclature for the central and northern North Sea. *Institute of Geology Scientific Report 77/25/ Norwegian Petroleum Directorate Bulletin 1,* 35 pp.

Dehandschutter, B., Vandycke, S., Sintubin, M., Vendenberghe, N. & Wouters, L. 2005: Brittle fractures and ductile bands in argillaceous sediments: inference from Oligocene Boom Clay (Belgium). Journal of *Structural Geology 27,* 1095–1112. https://doi.org/10.1016/j.jsg.2004.08.014.

Fraser, S.I., Robinson, A.M., Johnson, H.D., Underhill, J.R., Kadolsky, D.G.A., Connell, R., Johannessen, P. & Ravnås, R. 2003: Upper Jurassic. *In* Evans, D., Graham, C., Armour, A. & Bathurst, P. (eds.): *The Millennium Atlas: petroleum geology of the central and northern North Sea,* The Geological Society of London, pp. 157–189.

Gabrielsen, R.H. 1997: Procedures in core fracture logging. *Structural Geology Laboratory, University of Bergen, Report No. 16,* 19 pp.

Gabrielsen, R.H. & Aarland, R.K. 1990: Characteristics of pre- and synconsolidation structures and tectonic joints and microfaults in fine to medium-grained sandstones. *In* Barton, N. & Stephansson, O. (eds.): *Rock Joints*, Balkema, pp. 45–50.

Gabrielsen, R.H. & Braathen, A. 2014: Models of fracture lineaments – Joint swarms, fracture corridors and faults in crystalline rocks, and their genetic relations. *Tectonophysics 628*, 26–44. https://doi.org/10.1016/j.tecto.2014.04.022.

Gabrielsen, R.H. & Kløvjan, O.S. 1997: Late Jurassic- early Cretaceous caprocks of the southwestern Barents Sea: Fracture systems and rock mechanical properties. *In* Møller-Pedersen, P. & Koestler, A.G. (eds.): *Hydrocarbon seals - importance for exploration and production*, Norwegian Petroleum Society Special Publication 7, pp. 73–89. https://doi.org/10.1016/S0928-8937(97)80008-2.

Gabrielsen, R.H., Færseth, R.B., Steel, R.J. & Kløvjan, O.S. 1990: Architectural styles of basin fill in the northern Viking Graben. *In* Blundell, D. & Gibbs, A. (eds.): *Evolution of the North Sea Rifts,* Oxford Press, pp. 158–179.

Gabrielsen, R.H., Kyrkjebø, R., Faleide, J.I., Fjeldskaar, W & Kjennerud, T. 2001: The Cretaceous post-rift basin configuration of the northern North Sea. *Petroleum Geoscience 7,* 137–154. https://doi.org/10.1144/petgeo.7.2.137.

Gabrielsen, R.H., Braathen, A., Kjemperud, M. & Valdresbåten, M.L.R. 2017: The geometry and dimensions of fault core lenses, *Geological Society London, Special Publication 439,* 249–269. https://doi.org/10.1144/SP439.4.

Gale, J.F., Laubach, S.E., Olson, J.E., Eichhubl, P. & Fall, A. 2014: Natural fractures in shale: a review and observations. *American Association of Petroleum Geologists Bulletin 98,* 2165–2216. https://doi.org/10.1306/08121413151.

Glennie, K.W. (ed.) 1984: *Introduction to the Petroleum Geology of the North Sea.* Blackwell, London, 236 pp.

Gray, M.B. & Nickelsen, R.P. 1989: Pedogenic slickensides, indicators of strain and deformation processes in redbed sequences of the Appalachian foreland. *Geology 17,* 72–75. https://doi.org/10.1130/0091-7613(1989)017<0072:PSIOSA>2.3.CO;2.

Green, A.S.P., Baria, R., Madge, A. & Jones, R. 1988: Fault-plane analysis of microseismicity induced by fluid injection in granite. *In* Bell, F.G., Culshaw, M.G., Cripps, J.C. & Lovell, M.A. (eds.): *Engineering Geology of Underground Movements.* Engineering Geology Special Publication, Geological Society London 5, pp. 415–422. https://doi.org/10.1144/GSL.ENG.1988.005.01.46.

Halland, E.K., Johansen, W.T. & Riis, F. 2011: *CO_2 Storage. Atlas, Norwegian North Sea.* Norwegian Petroleum Directorate, Stavanger, 72 pp.

Hancock, P.L. & Barka, A.A. 1987: Kinematic indicators on active normal faults in western Turkey. *Journal of Structural Geology 9,* 573–584. https://doi.org/10.1016/0191-8141(87)90142-8.

Harrington, J.F., Cuss, R.J. & Talandier, J. 2017: Gas transport properties through intact and fractured Callovo–Oxfordian mudstone. *In* Rutter, E.H., Mecklenburgh, J. & Taylor, K.G. (eds.): *Geomechanical and Petrophysical Properties of Mudrocks,* Geologcal Society of London, Special Publication 454, pp. 131–154. https://doi.org/10.1144/SP454.7.

Heeremans, M. & Faleide, J.I. 2004: Late Carboniferous–Permian tectonics and magmatic activity in the Skagerrak, Kattegat and the North Sea. *In* Wilson, M., Neumann, E.-R., Davies, G.R., Timmerman, M.J., Heeremans, M. & Larsen, B.T. (eds.): *Permo–Carboniferous Magmatism and Rifting in Europe.* Geological Society of London Special Publication 223, pp. 157–176. https://doi.org/10.1144/GSL.SP.2004.223.01.07.

Hermanrud, C., Bolås, H.M.N. & Teige, G.M.G. 2005: Seal failure related to basin-scale processes. *In* Boult, P. & Kaldi, J. (eds.) 2005: *Evaluating Fault and Cap Rock Seals,* American Association of Petroleum Geologists, Hedberg Series 2, pp. 13–22.

Hettema, M.H.H., Hansen, T.H. & Jones, B.L. 2002: Minimizing coring-induced damage in consolidated rock. *Society of Petroleum Engineers SPE 78156,* 1–11. https://doi.org/10.2118/78156-MS.

Hill, D.G. & Nelson, C.R. 2000: Gas productive fractured shales – an overview and update. *GasTIPS 6,* 4–13.

Horsrud, P., Sønstebø, E.F., & Bøe, R. 1998: Mechanical and petrophysical properties of North Sea shales. *International Journal of Rock Mechanics and Mining Sciences 35,* 1009–1020. https://doi.org/10.1016/S0148-9062(98)00162-4.

IUGS 2018: *International Chronological Chart v2018/07.* https://stratigraphy.org/ICSchart/ChronostratChart2018-07.pdf (accessed 17. December 2020).

Kalani, M., Jahren, J., Mondol, N.H. & Faleide, J.I. 2015: Compaction processes and rock properties in uplifted clay dominated units – The Egersund Basin, Norwegian North Sea. *Marine and Petroleum Geology 68,* 596–613. https://doi.org/10.1016/j.marpetgeo.2014.08.015.

Keym, M., Dieckmann, V., Horsfield, B., Erdmann, M., Galimberti, R., Kua, L.-C., Leith, L. & Podlaha, O. 2006: Source rock heterogeneity of the Upper Jurassic Drapune Formation, North Viking Graben, and its relevance to petroleum generation studies. *Organic Geochemistry 37,* 220–243. https://doi.org/10.1016/j.orggeochem.2005.08.023.

Khan, T.J. 2013: *Structure and evolution of the Ling Depression and adjacent highs in the central North Sea.* Unpublished MSc thesis, University of Oslo, 93 pp.

Kirkpatrick, J.D. & Brodsky, E.E. 2014: Slickenline orientations as a record of fault rock rheology. *Earth and Planetary Science Letters 408,* 24–34. https://doi.org/10.1016/j.epsl.2014.09.040.

Kisch, H.J. 1991: Development of slaty cleavage and degree of very low grade metamorphism: a review. *Journal of Metamorphic Geology 9,* 735–750. https://doi.org/10.1111/j.1525-1314.1991.tb00562.x.

Kubala, M., Bastow, M., Thompson, S., Scotchman, I., Oygard, K., 2003. Geothermal regime, petroleum generation and migration. *In* Evans, D., Graham, C., Armour, A. & Bathurst, P. (eds.): *The Millennium Atlas: petroleum geology of the central and northern North Sea,* The Geological Society of London, pp. 289–315.

Kyrkjebø, R., Gabrielsen, R.H. & Faleide, J.I. 2004: Unconformities related to the Jurassic–Cretaceous syn/post-rift transition of the northern North Sea. *Journal of the Geological Society of London 161,* 1–17. https://doi.org/10.1144/0016-764903-051.

Ladéveze, P., S´journé, S., Rivard, C., Lavoie, D., Lefebre, R. & Rouleau, A. 2018: Defining the natural fracture network in shale gas play and its cover succession: The case of the Utica Shale in eastern Canada. *Journal of Structural Geology 108,* 157–170. https://doi.org/10.1016/j.jsg.2017.12.007.

Lindanger, M., Gabrielsen, R.H. & Braathen, A. 2007: Analysis of rock lenses in extensional faults. *Norwegian Journal of Geology 87,* 361–372.

Loucks, R.G., Reed, R.M., Ruppel, S.C. & Jarvie, D.M. 2009: Morphology, genesis, and distribution of nanometer-scale pores in siliceous mudstones of the Mississippian Barnett shale. *Journal of Sedimentological Research 78,* 848–861. https://doi.org/10.2110/jsr.2009.092.

Luo, X. & Vasseur, G. 1997: Sealing efficiency in shales. *Terra Nova 9,* 71–74. https://doi.org/10.1111/j.1365-3121.1997.tb00005.x.

Makurat, A., Tørudbakken, B., Monsen, K. & Rawlings, C. 1992: Cenozoic uplift and caprock seal in the Barents Sea: Fracture modelling and seal risk evaluation. *Society of Petroleum Engineers SPE 24740,* 821–830. https://doi.org/10.2118/24740-MS.

Maltman, A.J. 1981: Primary bedding-parallel fabrics in structural geology. *Journal of the Geological Society London 138,* 475–483. https://doi.org/10.1144/gsjgs.138.4.0475.

Means, W.D. 1987: A newly recognized type of slickenside striation. *Journal of Structural Geology 9,* 585–590. https://doi.org/10.1016/0191-8141(87)90143-X.

Mondol, N.H., Bjørlykke, L., Jahren, J. & Høeg, K. 2007: Experimental mechanical compaction of clay mineral aggregates – Changes in physical properties of mudstones during burial. *Marine and Petroleum Geology 24,* 289–311. https://doi.org/10.1016/j.marpetgeo.2007.03.006.

Nelson, R.A., 2001: *Geologic Analysis of Naturally Fractured Rocks. 2nd* Edition, Gulf Publishing, Book Division, 332 pp.

Nordgård Bolås, H.M., Hermanrud, C. & Teige, G.M. 2005: Seal capacity estimation from subsurface pore pressures. *Basin Research 17,* 583–599. https://doi.org/10.1111/j.1365-2117.2005.00281.x.

Norwegian Petroleum Directorate 2014: *NPD Factpages*. https://factpages.npd.no/ (accessed 17. December 2020).

Nøttvedt, A., Gabrielsen, R.H. & Steel, R.J. 1995: Tectonostratigraphy and sedimentary architecture of rift basins, with reference to the northern North Sea. *Marine and Petroleum Geology 12*, 881–901. https://doi.org/10.1016/0264-8172(95)98853-W.

Odling, N.E., Gillespie, P., Bourgine, B., Castaing, C., Chilés, J.-P., Christensen, N.P., Fillion, E., Genter, A., Olsen, C., Thrane, L., Trice, R., Aarseth, E., Walsh, J.J. & Watterson, J. 1999: Variations in fracture system geometry and their implications for fluid flow in fractured hydrocarbon reservoirs. *Petroleum Geoscience 5,* 373–384. https://doi.org/10.1144/petgeo.5.4.373.

Ogebule, O.Y. 2015: Analysis Core 1, 11 pp. *In* Skurtveit, E. & Soldal, M. (eds.): *Geomechanical test program on the Draupne shale core material, Well 18/8-3,* NGI Report, 20140434-01-R.

Ogier-Somoin, A., Renard, F., Boehm, C. & Vidal-Gilbert, S. 2016: Microfracturing and microporosity of shales. *Earth-Science Reviews 162*, 198–226. https://doi.org/10.1016/j.earscirev.2016.09.006.

Petit, J.P. 1987: Criteria for the use of movement on fault surfaces in brittle rocks. *Journal of Structural Geology 9*, 597–608. https://doi.org/10.1016/0191-8141(87)90145-3.

Power, W.L. & Tullis, T.E. 1989: The relationship between slickenside surfaces in fine-grained quartz and the seismic cycle. *Journal of Structural Geology 11,* 879–893. https://doi.org/10.1016/0191-8141(89)90105-3.

Rawson, P.F. & Riley, L.A. 1982: Latest Jurassic - early Cretaceous events and the "Late Cimmerian Unconformity" in North Sea area. *American Association of Petroleum Geologists Bulletin 66,* 2628–2648. https://doi.org/10.1306/03B5AC87-16D1-11D7-8645000102C1865D.

Renard, F., Mair, K. & Gundersen, O. 2012: Surface roughness evolution on experimentally simulated faults. *Journal of Structural Geology 45,* 101–111. https://doi.org/10.1016/j.jsg.2012.03.009.

Ross, D.J.K. & Bustin, R.M. 2008: Characterizing the shale gas resource potential of Devonian-Mississippian in the western Canada sedimentary basin: application of an integrated formation evaluation. *American Association of Petroleum Geologists, Bulletin 92*, 87–125. https://doi.org/10.1306/09040707048.

Rutter, E.H. & Mecklenburgh, J. 2017: Hydraulic conductivity of bedding-parallel cracks in shale as a function of shear and normal stress. *In* Rutter, E.H., Mecklenburgh, J. & Taylor, K.G. (eds.): *Geomechanical and Petrophysical Properties of Mudrocks,* Geological Society London Special Publication 454, pp. 305–326. https://doi.org/10.1144/SP454.16.

Schueller, S., Braathen, A., Fossen, H. & Tveranger, J. 2012: Fault damage zones of extensional faults in porous sandstone: spatial distribution of deformation bands. *Journal of Structural Geology 52,* 148–162. https://doi.org/10.1016/j.jsg.2013.03.013.

Sibson, R.H. 1990: Faulting and fluid flow. *In* Nesbitt, B.E. (ed.): *Short course on fluids in tectonically active regions of the continental crust,* Mineralogical Association of Canada, Handbook 18, pp. 93–132.

Skurtveit, E., Aker, E., Soldal, M., Angeli, M. & Wang, Z. 2012: Experimental investigation of CO_2 breakthrough and flow mechanisms in shale. *Petroleum Geoscience 18,* 3–15. https://doi.org/10.1144/1354-079311-016.

Skurtveit, E., Grande, L., Ogebule., O.Y., Gabrielsen, R.H., Faleide, J.I., Mondol, N.H., Maurer, R. & Horsrud, P. 2015a: Mechanical testing and sealing capacity of the Upper Jurassic Draupne Formation, North Sea. *Proceedings 49th US Rock Mechanics / Geomechanics Symposium ARMA15-331,* 1–8.

Skurtveit, E., Torabi, A., Alikarini, R. & Braathen, A. 2015b: Fault baffle to conduit developments: reactivation and calcite cementation of deformation bad fault in aeolian sandstone. *Petroleum Geoscience 21,* 3–16. https://doi.org/10.1144/petgeo2014-031.

Thyberg, B. & Jahren, J. 2011: Quartz cementation in mudstones: sheet-like quartz cement from clay mineral reactions during burial. *Petroleum Geoscience 17,* 53–63. https://doi.org/10.1144/1354-079310-028.

Thyberg, B., Jahren, J., Winje, T., Bjørlykke, K. & Faleide, J.I. 2009: From mud to shale: rock stiffening by micro-quartz cementation. *First Break 27*, 27–32. https://doi.org/10.3997/1365-2397.2009003.

Tingay, M., Reinecker, J. & Müller, B. 2008: *Borehole breakout and drilling-induced fracture analysis from image-logs, Guide-line: Image logs.* World Stress Map Project, 8 pp.

Toy, V.G., Niemeijer, A., Renard, F., Morales, L. & Wirth, R. 2017: Striation and slickenline development on quartz fault surfaces at crustal conditions: Origin and effect on friction. *Journal of Geophysical Research, Solid Earth 122,* 1–16. https://doi.org/10.1002/2016JB013498.

Twiss, R.J., Protzmann, G.M. & Hurst, S.D. 1991: Theory of slickenline patterns based on the velocity gradient tensor and microrotation. *Tectonophysics 186,* 215–239. https://doi.org/10.1016/0040-1951(91)90360-5.

van den Berg, L. 1987: Experimental redeformation of naturally deformed scaly clays. *Geologie en Mijnbouw 65,* 309–325.

Vollset, J. & Doré, A. 1984: *A revised Triassic and Jurassic lithostratigraphic nomenclature for the North Sea.* Norwegian Petroleum Directorate Bulletin 3, 53 pp.

Warren, J.K., Cheung, W. & Cartwright, I. 2010: Organic geochemical, isotopic, and seismic indicators of fluid flow in pressurized growth aniticlines and mud volcanoes in modern deep-water slope and rise sediments of offhsore Brunei Darussalam: implivarions for hydrocarbon exploration and other mud- and salt-diapir provinces. *In* Wood, L.J. 2010 (ed.): *Shale Tectonics,* American Association of Petroleum Geologists Memoir 93, pp. 163–196. https://doi.org/10.1306/13231314M933424.

Watts, N.L. 1987: Theoretical aspects of caprock and fault seals for single- and two-phase hydrocarbon columns. *Marine and Petroleum Geology 4,* 274–307.

Weatherford Laboratories 2013: *Statoil Well 16/8–s;* Scan series April 17, 2013, 10 pp.

Whitbread, D.R. 1975: Geology and petroleum possibilities west of the United Kingdom. *In* Woodland, A.W. (ed.): *Petroleum and the continental shelf of North–West Europe,* John Wiley & Sons, pp. 45–60.

Will, T.M. & Wilson, C.J.L. 1989: Experimentally produced slicken side lineation in poryphyllitic clay. *Journal of Structural Geology 11*, 657–667. https://doi.org/10.1016/0191-8141(89)90002-3.

Wilson, C.J.L. & Will, T.M. 1990: Slickenside lineations due to ductile processes. *In* Knipe, R.J. & Rutter, E.H. (eds.): *Deformation Mechanisms, Rheology and Tectonics,* Geological Society of London, Special Publication 54, pp. 455–460. https://doi.org/10.1144/GSL.SP.1990.054.01.41.

Wood, L.J. (ed.) 2010a: *Shale Tectonics.* American Association of Petroleum Geologists Memoir 93, 238 pp.

Wood, L.J. 2010b: Shale tectonics: A preface. *In* Wood, L.J. 2010 (ed.): *Shale Tectonics,* American Association of Petroleum Geologists Memoir 93, pp. 1–4.

Yarushina, V.M. 2018: Potential leakage mechanisms and their relevance to CO_2 storage site risk assessment and safe operations. FME SUCCESS *Synthesis report Volume 2, SUCCESS Technical Report,* 31 pp.